Semi continuous thermochemical reactor for thermal storage

Joël Wyttenbach[1], Gilbert Descy[2] and Alexandre Descy[2]
[1] Univ. Grenoble Alpes, F-38000 Grenoble, France. CEA, LITEN, F-38054 Grenoble, France
[2] BESOL, rue de la Griotte, 2a, 5580 Rochefort, Belgium

Abstract

A new semi-continuous thermochemical reactor prototype for seasonal heat storage was designed, manufactured and tested. Its cross flow vertical moving bed design improves a combination of performance factors, including energy density, heat power, temperature level, reversibility, thermal losses and auxiliary consumption. Tests were conducted on a dynamically controlled air flow equipment where a calibrated instrumentation allowed measuring thermal power with temperature and humidity methods, in addition to mass gradients.

After an initialization phase, the reactor works semi-continuously and heat power shows only small variations. It was measured at 415 W in both modes, and is almost proportional to air flow rate, while coefficient of performance is excellent (19 to 45). Those results were confirmed by two distinct measurement methods, based alternately on temperature and humidity. Charging phase could be performed at only 60.3°C, which is a major result because it leads to increasing system efficiency of solar thermal storage systems. Besides, it was highlighted that a better reaction real time monitoring would ease the control and increase performance, especially regarding energy density. Temperature maps were installed on both sides of the reacting bed. Results suggest that beyond the qualitative results, they could be used to calculate a real time distribution of composite hydration level.

Keywords: Thermochemical reactor, Semi-continuous, Performance test, Seasonal storage, Space heating

1. Introduction

On a yearly basis, a limited solar collector surface is able to produce enough energy to meet heating needs of a building in a temperate climate. However, solar resource is mostly not available during winter season, which is why a long term storage is required to fully take advantage of the annual solar irradiation (Letz, 2002). In this context, thermochemical technology offers very interesting energy density and almost no long term thermal losses compared to sensible and even phase change storage methods (Marias, 2015). Indeed, energy is stored as a chemical potential within a solid material that is alternately hydrated and dehydrated through respectively exo- or endothermic reactions.

Setting up an appropriate reversible reactor is of a major importance in order to optimize heat storage and generation. Indeed, the challenge is to increase the mass transfer rate between water vapor and solid hydrate, while controlling outlet heat power and minimizing electrical consumption.

This article describes a new reactor type that was designed to answer the needs of thermochemical seasonal heat storage. Its tested performances are discussed in this context.

2. Prototype presentation

As pure water is not available in gaseous phase at atmospheric pressure and space heating temperature, thermochemical reactors usually work either at low pressure or with moist air water content (Michel et al., 2012). In the first case, water has to be either stored in an expansive low pressure vessel or dynamically generated with consistent energy consumption. Although several low pressure reactor types were designed and tested by various research teams (Van Helden et al., 2014) (Mauran et al., 2008), their technical complexity is usually quite high in the context of building industry.

In the second reactor concept, moist air moves water and heat to and from solid hydrate, which allows to work at atmospheric pressure. Water storage is therefore optional since it is possible to work with outside air, as long as water content fluctuation can be dealt with. In addition, this configuration allows to separate solid hydrate storage and reactor location since it is easier to design a conveying device working at atmospheric pressure. With this separation concept, both reactant flows can be controlled in order to optimize reaction process. Given this degree

doi:10.18086/eurosun2018.13.07 Available at http://proceedings.ises.org

of freedom, the goal is to find the best compromise between power, energy and exergy performance factors. A first step is to describe what influences these factors.

- Heat power increases with
    - Better reaction kinetics
    - Higher transfer rates in the heat carrier exchangers.
    - Larger cross section on air flow
    - Counterflow or crossflow configuration
    - Continuous solid flow
- Thermal energy stored or restituted increases when hydration level difference increases between dehydrated and hydrated phases of solid material. Electrical energy consumption decreases when reactants' flows are facilitated.
- Exergy performance reaches its target when heat carrier temperature is high enough to ensure sufficient heat transfer to the building.

Solid/gas thermochemical reactors also have to adapt to the very high volume difference between reactants, especially when they work with moist air, as the gaseous reactant is diluted in the heat carrier. Thermodynamically, this dilution also lowers maximum outlet temperature, which requires to reduce exergy losses.

These specific requirements lead to design a crossflow vertical moving bed reactor operating with semi continuous solid flow and atmospheric moist air.

This reactor is made of a narrow 8 mm wide cavity limited by two vertical metallic sieves and a bottom valve. The moist air flow runs through the solid material located in the cavity, its movement is facilitated by a generous 0.36 m² cross section and a limited depth. Solid material flows downwards thanks to gravity and the bottom valve controls its speed so that only a fraction of the load is replaced at each open/close cycle, which defines a semi-continuous working principle. With a 520 mm height, solid material path is 65 times longer than gaseous one. This helps reducing the reactants' volume difference impact, leading to a better energy performance. The upper opening of the reactor communicates with a small reservoir filled with solid reactant that makes the vessel practically airtight. The solid material used is made of a silica gel matrix impregnated with around 43 wt % of Calcium Chloride ($CaCl_2$). The synthesis method and the characterization tests were described by Courbon et al (Courbon et al., 2017) for different patented composites (Courbon et al., 2015)

When air flows through the reactor, it carries water vapor molecules either to or from the solid material. This happens respectively when an exothermic water adsorption reaction or an endothermic desorption reaction takes place (Mette et al., 2014). Air acts as heat carrier in both cases, which is why the reactor is well insulated and airtight.

Since solid material needs to move slowly, the reactor control works with open/close cycles that allow to drain approximately one sixth of the full load at each opening, which defines a reaction step. New solid material enters the reactor through the upper opening thanks to gravity.

The reactor illustrated on Figure 1 relies on efficient convective mass- and heat transfers that increase its generated power. As an example of technical compromise, the air pressure drop through the solid bed is high enough to create an even velocity distribution across the section plane, leading to a better exergy performance, while it is low enough to limit auxiliary power consumption, leading to a better energy performance.

While taking into account the above mentioned criteria, the reactor's type and shape remain quite similar to thermochemical systems found in the literature, as described for example by Kerskes et al (Kerskes et al., 2012), Bonk et al. (Bonk et al., 2017) and Nonnen et al. (Nonnen et al., 2016). However, the reactor bed's thickness is particularly thin compared to references mentioned above, which is a major asset to lower air pressure drop and the auxiliary electrical consumption. In addition, some design decisions were taken to keep technical realization simple, for example regarding crossflow rather than counterflow configuration. Therefore, it was decided to test the reactor in order to assess its actual performances and to identify practical use issues.

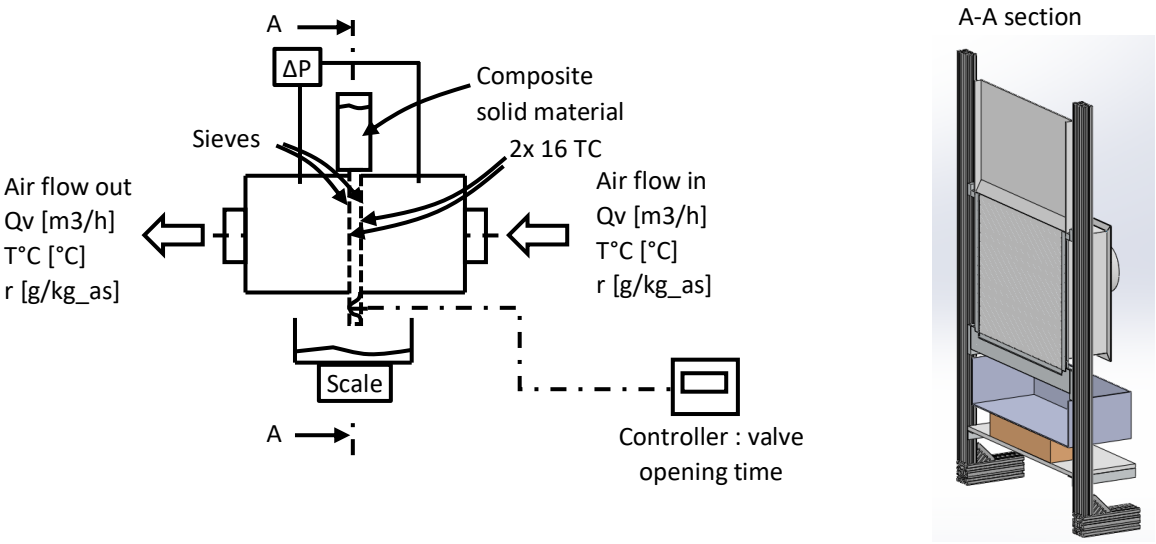

Figure 1 – Semi continuous cross flow reactor

Prior to testing the reactor, solid flow control issues need to be discussed. Indeed, reactor's first load is entirely made of "new" composite: for a hydration reaction, the initial solid material load is entirely dehydrated. This is not the case anymore in continuous operation mode: the horizontal layers are increasingly hydrated on the way down, for a hydration reaction. This means that reaction starts with an initialization period during which time heating or cooling power is greater. Then, power stabilizes after a certain amount of partial draining, and when outlet temperature and humidity remain constant for two consecutive steps, we consider that the semi continuous phase starts.

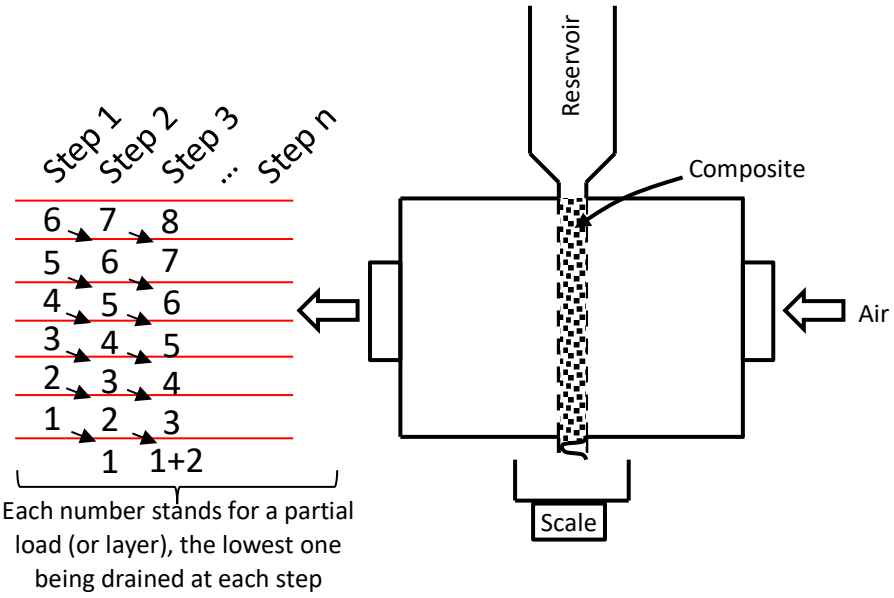

Figure 2 – Control of a semi continuous reactor

This cross flow vertical reactor is a volumetric machine, which induces that each step should be defined as a fraction of total reactive volume, as it is suggested on Figure 2. For technical reasons, a time based valve is rather installed, and exiting solid mass is measured with a weighing scale. Not having the volume information requires additional calculations: a real time water vapor mass counter is setup using specific humidity measurements (Equation 1). Then, a target mass uptake is calculated (Equation 2) so that the solid material reaches the forecasted final hydration level. Water vapor mass counter is initialized after each draining. When it reaches the value described by Equation 3, a new partial draining takes place. The solid mass $M_{drained}$ [kg] to be drained at one step is given by Equation 4.

$$\Delta M_{water}(t) = \int_{t=0}^{t} \dot{m}_{dry\ air}.(w_i - w_o).dt$$

Equation 1

$$\Delta M_{water\_expected} = M_{solid_{anhydrous}}(\mathrm{X}_{final_{expected}} - \mathrm{X}_{initial})$$

Equation 2

$$\Delta M_{water}(t_d) = \frac{\Delta M_{water\_expected}}{Number\ of\ steps}$$

Equation 3

$$M_{drained} = \frac{M_{solid_{anhydrous}} * \left(1 + \mathrm{X}_{final_{expected}}\right)}{Number\ of\ steps}$$

Equation 4

Where $\Delta M_{water}(t)$ [kg] is water mass uptake, $\dot{m_{dry\ air}}$ [kg/s] is dry air mass flow, w_i and w_o [kg/kg$_{da}$] are reactor inlet and outlet air specific humidity, $\Delta M_{water\_expected}$ [kg] is expected water mass uptake, $M_{solid\_anhydrous}$ [kg] is the mass of the solid in its anhydrous state, $X_{final\_expected}$ [kg/kg] is expected solid composite final hydration level, t_d [s] is the time when partial draining occurs and Number of steps [-] is the amount of steps needed to fully drain the reactor.

However, this control scheme is global rather than a layer per layer approach. To compare real time counter results to a reference, exiting solid material hydration level is characterized with a moisture analyzer. This comparison helps increasing the team's know-how regarding reactor control, but test conditions are still not perfectly replicable, which is why results have to be analyzed carefully.

The solid flow management issue highlights that mass measurement is less appropriate than volume to control such reactor type. Furthermore, individual layer hydration level is difficult to calculate accurately, especially in a realistic environment with variable air inlet conditions. This highlights the need of an advanced instrumentation able to provide a reactor load hydration level map in real time. We also note that the reactor behaves quite differently during initialization phase, which is why initialization's occurrence has to be minimized.

3. Test method

Test setup

The objective of the tests is to measure reactor's power and energy during at least one period of semi-continuous operation. It is also important to measure temperature elevation in order to define potential application of the technology. To do this, the reactor is connected to the MATher test equipment that prepares the air flow at the expected temperature and humidity ratio. Reactor performances are measured with following instrumentation setup:

- Inlet and outlet humidity ratio and air flow rate are measured with high accuracy sensors, as part of permanent and periodically controlled MATher test equipment. Air flow relies on vortex speed sensors and humidity on best-in-class capacitive sensors.
- Reactor inlet and outlet temperatures are measured with 6 calibrated thermocouples
- Solid bed inlet and outlet temperatures are measured with 32 calibrated thermocouples spread over inlet and outlet sieves.
- Solid composite exiting reactor is monitored in real time with a weighing scale for flow control issues. Entering and exiting solid composite mass is measured by a second weighing scale with a finer resolution for better metrological results.
- A differential pressure sensor measures the reactor pressure drop in order to calculate a realistic coefficient of performance.

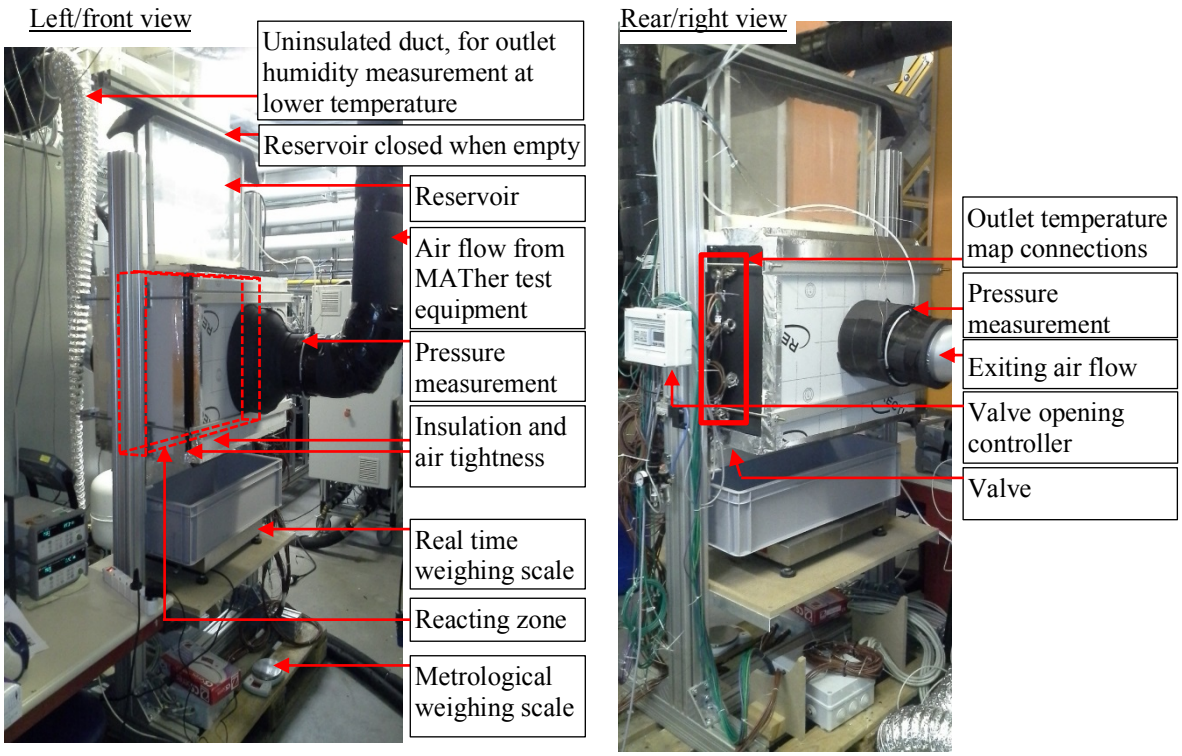

Figure 3 – Reactor connected to the test equipment, with specific instrumentation

Moving solid may induce uneven reactor behavior within the air flow cross section. Therefore, 16 temperature sensors are installed on each side of the solid material vertical bed in order to check locally if the reactor behaves as expected. Indeed, a temperature map is greatly influenced by air flow rate, hydration level or thermal losses disorders. Moreover, temperature maps allow to check experimentally if expected behavior can be actually observed, which is a vertical gradient and constant values along horizontal lines.

Higher dehydration temperatures (up to 90.9°C) raise a problem about humidity measurement, as commonly used capacitive or dew point sensor technologies are better suited to temperatures below 40°C. For this reason, two specific measuring configurations are setup:

- Inlet humidity is measured further up on the air flow line of MATher test equipment, where air temperature never exceeds 40°C. Downstream, a final heating stage allows to increase temperature to the expected level with no effect on humidity content.
- Outlet humidity measurement needs to be performed after an air flow cooling stage, which is not implemented on the well-insulated outlet lines. Therefore, a long uninsulated duct is added between reactor outlet and permanent outlet lines in order to cool the air flow by yielding heat to the ambience. Dimensioning is performed experimentally to reach enough cooling without any condensation risk.

Test conditions

Testing conditions and the statistical approach to select them are reported on Table 1. Calculations are performed with following parameters:

- Brussels climate with extreme and mid-season cases
- A 16 m² area of flat solar thermal panel, for dehydration temperature calculation
- Constant air flow rate for first performance tests, as it is a function of reactor cross section.
- Variable air flow rate in hydration mode for sensitivity analysis
- Constant temperature in hydration mode: we suppose that the house is provided with an air recovery heat exchanger. The reactor is located downstream on the fresh air flow line.

Dehydration temperature comes from dynamic thermal simulation

Table 1 – Inlet temperature and humidity test conditions

Mode	T_{in} [°C]	r_{in} [g/kg$_{da}$]	Q_v [kg/m^3]	Reference	Statistical approach
Hydration	20.2	4	120	Winter	Most frequent humidity when $T_{outside}$ is between -1 and +1°C
Hydration	20.2	9	120	Mid season	Most frequent humidity when $T_{outside}$ is between 14 and 16°C
Dehydration	60.3	4	120	Early spring	Most frequent day humidity in March
Dehydration	76.5	6	120	Mid season	Most frequent day humidity over March to May plus September period
Dehydration	90.5	11.5	120	Summer	Most frequent day humidity in August
Hydration	20.2	4	75	Winter	Most frequent humidity when $T_{outside}$ is between -1 and +1°C
Hydration	20.2	4	102	Winter	
Hydration	20.2	4	152	Winter	

Where T_{in} [°C] is inlet air temperature, r_{in} [g/kg$_{da}$] is inlet air specific humidity and Q_v [kg/m^3] is air volume flow rate.

4. Experimental results

Hydration

The hydration test with air inlet conditions at 20.2°C, 3.9 g/kg$_{da}$ and 122 kg/h is shown on Figure 4 with its initialization phase. We see that heat power is higher at the beginning of the test, when the whole reactor is filled with dry composite. Then, the solid load moves downwards at each partial draining step, which finally creates a hydration level vertical gradient. Consequently, heat power decreases and stabilizes. The second highlighted period can be therefore considered as semi-continuous operation.

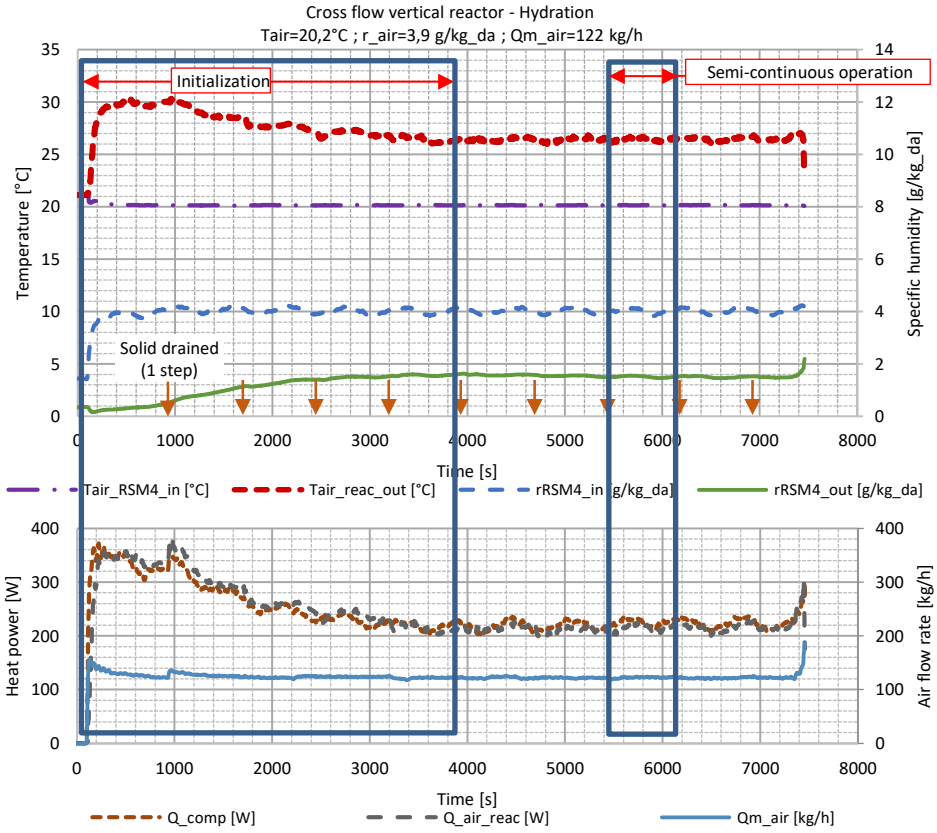

Figure 4 – Full hydration test, with initialization phase

Where Tair_RSM4_in [°C] is air temperature at reactor inlet, Tair_reac_out [°C] is air temperature at reactor outlet, Qm_air [kg/h] is air mass flow rate, rRSM4_in [g/kg$_{da}$] is air specific humidity at reactor inlet, rRSM4_out [g/kg$_{da}$] is air specific humidity at reactor outlet, Q_comp [W] is heating/cooling power measured on the

composite, and Q_air_reac [W] is heating/cooling power measured on the air.

Hydration heat power is quite stable during the one step period of semi-continuous operation highlighted on Figure 4. Besides, the two calculation methods (temperature and humidity) provide very close results, although heat power is slightly lower with temperature method, probably because thermal losses are taken into account. This confirms that the measurement method is adapted to calculate reactor's heat power.

In order to further analyze performances, indicators presented on Table 2 and reported on Table 3 are averaged over the duration of one step period, between two draining.

Table 2 – Performance indicators description

Indicator	Unit	Parameter description
ΔTair	[K]	Average* air temperature variation through reactor
Δr	[g/kg$_{da}$]	Average* air humidity ratio variation through reactor
ΔP	[Pa]	Average* reactor air pressure drop
Xinit	[-]	Initial composite hydration level, measured with moisture analyzer
Xfinal_150°C	[-]	Final composite hydration level, measured with moisture analyzer
Δm_{vapor}	[g]	Water vapor mass transferred, measured on air humidity
E_Density	[Wh/kg]	Energy density measured on air temperature
Q_air	[W]	Heating power, measured on air temperature
COP	[W/W]	Ratio Q_air/Q_elec, with Q_elec=f(ΔP ;Qm_air)

*Average over the duration of a reactor step between two solid draining in semi continuous operation

Table 3 – Hydration performance indicators

Test ID	Hydration 20.2°C, 3.9 g/kg$_{da}$, 122 kg/h	Hydration 20.2°C, 9 g/kg$_{da}$, 118 kg/h	Hydration 20.2°C, 4.1 g/kg$_{da}$, 90 kg/h	Hydration 20.2°C, 4.2 g/kg$_{da}$, 122 kg/h	Hydration 20.1°C, 4.1 g/kg$_{da}$, 182 kg/h
ΔTair [K]	6,08	12,61	4,93	5,78	5,3
Δr [g/kg$_{da}$]	-2,5	-5,03	-1,92	-2,64	-2,12
ΔP [Pa]	112,9	98,4	89,7	115,2	187,6
Xinit	9,3%	9,5%	10,2%	10,2%	10,2%
Xfinal_150°C	34,4%	*31.55%**	41,0%	36,7%	41,7%
Δm_{vapor} [g]	64,1	57,6	56,4	87,5	118,1
E_Density [Wh/kg]	161,7	139,2	146,6	221,8	260,5
Q_air [W]	214,9	415,1	128,9	195,8	275,7
COP [W/W]	19,48	45,1	19,35	17,56	10,17

*Uncertain measurement

Hydration heat power is almost twice when air inlet humidity increases from 3,9 to 9 g/kg$_{da}$. However, it is important to note that the 9 g/kg$_{da}$ test was stopped too early, which explains why final hydration ratio is not high enough. With a longer test, final hydration levels would be similar and it is likely that the heating power difference would be slightly less pronounced.

Hydration coefficient of performance (COP) is very high (up to 45), which means that reactor design decisions really lead to minimizing auxiliary electrical power.

The energy density is not an accurate measurement as it is measured on the full reactor load and given on Table 3 for only a partial load. Therefore, it is more relevant to consider final hydration ratio for energy density purposes. Each time solid material exits reactor with a water content below 40%, energy density is less than expected. This is the case for the 3.9 g/kg$_{da}$ test as this partial load was drained too early. Indeed, with limited real time monitoring means, the reactor control was not optimized yet. A longer reaction would bring energy density back to its expected value, while this would slightly reduce averaged heating power.

Air flow variations impact is shown on the 3 right columns of Table 3. Heat power tends to be a linear function of air flow rate: twice the air flow means approximately twice the heat power, but also approximately half the

COP (coefficient of performance). This means that reactor power modulation is possible through air flow control, with the limitation of electrical consumption. However, it is important to note that comparing those latter tests can be misleading because the hydration level distribution within the reactor is not well known. Indeed, it is likely that the three tests show different distributions, which affects heat power even if all other parameters are constant.

Energy density indicator is extrapolated considering a perfect semi-continuous operation with constant inlet conditions. However, air flow rate variations effects are measured during a single test without initialization between measurement steps. As a consequence, energy density results cannot be interpreted.

Although hydration global results are very interesting for space heating application, there is a need to better monitor the solid hydration level distribution within a reactor load, for control and performance optimization. Looking at the inlet and outlet temperature maps provide interesting information about how the reactor works. Table 4 shows outlet temperature map averaged over one step duration between two solid draining in semi-continuous phase, for adsorption test at 20.2°C, 3.9 g/kg$_{da}$ and 122 kg/h. Sensor locations are illustrated on Figure 5.

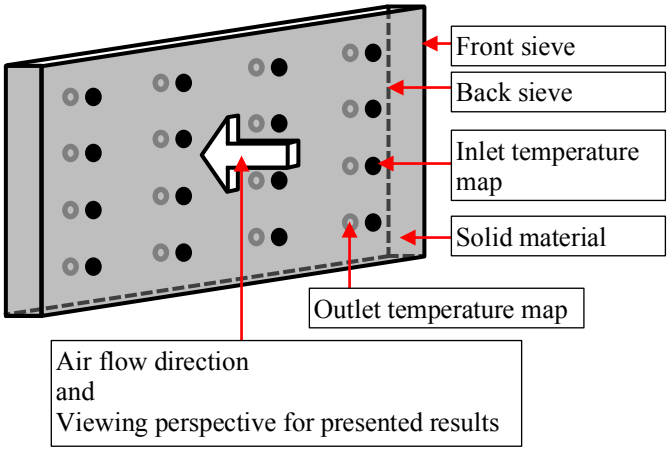

Figure 5 - Sensor spatial distribution in the temperature maps

Table 4 – Reactor outlet temperature map during hydration at 20.2°C, 3.9 g/kg$_{da}$ and 122 kg/h

Reactor outlet time averaged temperature map [°C]

29,7	29,2	29,1	30,2
26,1	29,4	27,4	28,0
25,5	26,4	25,8	26,2
23,4	25,5	25,4	25,7

Standard deviation over time of reactor outlet temperatures [K]

0,6	0,5	0,6	0,8
0,1	0,2	0,2	0,2
0,1	0,1	0,2	0,1
0,1	0,2	0,1	0,2

Adsorption outlet temperature is higher on the upper part of the reactor. Indeed, upper layer solid material is less hydrated than lower layer one, since it stayed in the reactor for a shorter time, its reaction kinetic is therefore higher for a given entering absolute humidity. We also note that temperatures are comparable on horizontal lines. These two expected results are now measured, which means that reactor's qualitative behavior matches with theoretical approach.

The standard deviation over time highlights that the lower temperatures are stable while upper layer shows more variation. Again, upper layer reacts faster, which slightly modifies solid material hydration level during one

reaction step. Therefore, upper outlet temperature shows a slight decrease during the selected time step.

Beyond the qualitative information given by the temperature map, we can note that each outlet temperature is a function of inlet air conditions and solid material hydration level. All other parameters being measured, it is possible to solve a thermodynamic equation system in order to compute the local hydration level of solid material facing each temperature measurement. As stated earlier, the availability of a real time hydration level map would be a great improvement, as solid flow would be controlled with a much better precision. Draining would occur only when a layer reaches its target hydration level, just below clogging limit, which is a key for a better energy density, a better storage management and less dysfunction.

Dehydration

The entire dehydration test with air at 60.3°C, 4 g/kg_{da} and 124 kg/h is presented on Figure 6. First, we see that the semi-continuous phase may have never been reached during the test, solid composite material quantity being limited.

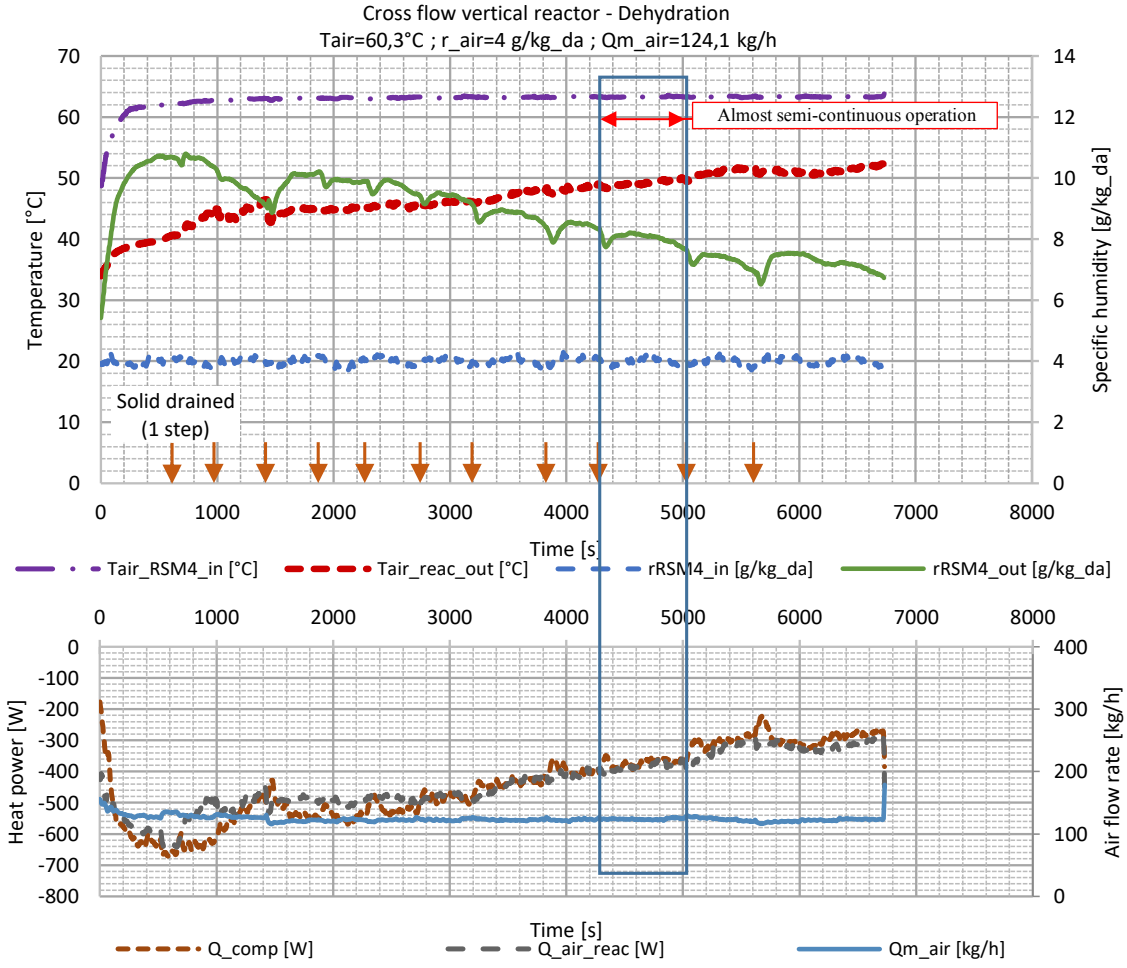

Figure 6 – Full dehydration test, with initialization phase

The stabilization time is indeed much longer than expected (≥1h45), based on what was measured in hydration mode (≈1h). As a consequence, the detailed one step analysis was performed before full stabilization, which means that following results have to be understood as almost but not exactly semi-continuous operation.

New solid material entering the reactor is much colder than the rest of the reacting load. Therefore, average temperature decreases at each partial drain/load, which explains that the reaction efficiency is lowered at the beginning of the highlighted step (Figure 6) for approximately 2 minutes. Then, heat power increases and stabilizes for more than 3 minutes before decreasing again due to slower reaction of dehydrated composite.

Cooling power calculated using temperature or humidity methods are very close, which confirms that the measurement setup is adapted to high temperature air flow. Thermal losses induce a slightly higher power for the temperature based calculation.

Table 5 presents the average performance indicators for three different dehydration tests. Cooling power is highly influenced by inlet conditions, and globally in the range of hydration heat power. Dehydration cooling power tends to increase with higher inlet temperature, but it also tends to decrease with higher inlet humidity ratio, at a given air flow rate and composite hydration level. Although this result was expected from thermodynamic equilibrium, it was not easy to highlight it on former prototypes. The 385 W cooling power at 60.3°C and 4 g/kg_{da} is also an interesting result as it shows that consistent dehydration process is possible even at a modest temperature in the context of solar thermal flat panel heat.

Table 5 - Dehydration performance indicators

Test ID	Dehydration 60.3°C 4 g/kg_{da} 124 kg/h	Dehydration 76.4°C 6 g/kg_{da} 122 kg/h	Dehydration 90.9°C 11 g/kg_{da} 122 kg/h
ΔTair [K]	-14,61	-11,8	-16,38
Δr [g/kg_{da}]	4,08	2,63	4,21
ΔP [Pa]	163,6	172	146,2
Xinit	40,3%	39,3%	40,0%
Xfinal_150°C	17,6%	18,4%	16,1%
Δmvapor [g]	-107,6	-86,7	-101,3
E_Density [Wh/kg]	247,9	208,7	250,9
Q_air [W]	-384,5	-289,2	-415,3
COP [W/W]	21,51	15	24,46

Again, the lack of solid material hydration level information disturbs reaction control. Therefore, expected final hydration level of 10% is not reached on exiting solid material because reaction is stopped too early.

In addition, the exiting solid does not always flow evenly, which means that some clogging occurs in the reactor, inducing different vertical solid speeds. Since clogging issues were reported especially for the 76,4°C dehydration test, its outlet temperature map is presented on Table 6.

Table 6 - Reactor outlet temperature map during dehydration at 76.4°C, 6 g/kg_{da} and 122 kg/h

Reactor outlet average temperature map [°C]

71,0	70,8	69,4	66,4
73,7	68,4	60,0	65,8
74,4	70,1	72,0	69,4
74,0	64,6	65,2	63,9

Standard deviation of reactor outlet temperatures [K]

0,2	0,2	0,3	0,3
0,2	0,4	0,7	1,5
0,2	0,6	1,1	2,8
0,1	1,0	0,5	0,4

The left temperature column is 6 K warmer than the rest of the reactor. As it is shown in the literature (Michel et al., 2016) (Marias, 2015), fixed bed reactors' cooling power decreases with time, therefore outlet temperature increases. Since this left column acts as if it was a fixed bed, it means that solid does not move anymore, probably because it is clogged.

Despite higher temperatures, inlet spatial standard deviation is under 1.3 K for all three dehydration tests. This shows that thermal insulation performance is good enough, otherwise cold walls would increase temperature differences. However, outlet standard deviations along some horizontal lines are well above 5 K. Left column is

even 10 K warmer than the rest for the 90.9°C dehydration test. This obvious clogging is not fully investigated yet, but there are at least two hypothesis:

- Solid material enters the reactor at ambient temperature. Because of its inertia, its cooling effect on the air is much more important at the beginning of the test. Consequently, air temperature might drop under the limit where hydration occurs. Solid material being already hydrated at about 40%, it is possible that a solution appears, clogging the reactor.
- As it is mentioned in the literature about fixed bed thermochemical reactors (Marias, 2015), reaction front is quite steep, meaning in our case that air reacts first with the first solid column it crosses. This reaction cools the air while increasing its specific humidity, which brings it closer to the thermodynamic hydration/dehydration limit. If for any reason the downstream solid material columns are more hydrated or colder, hydration can occur, and liquid solution appears, clogging the reactor

5. Conclusion

Based on previous work regarding integrated and separated moist air thermochemical systems (Pardo et al., 2014) (Wyttenbach et al., 2014), a new reactor concept was designed, manufactured and tested in order to improve not only one but a combination of three main performance factors that are energy, heat power, and exergy in both heating and storage modes. The new prototype works with moist air and is a cross flow vertical moving bed separate reactor operating semi continuously. The solid material load doesn't move during a reaction period, then only the lowest fraction is drained while the rest of the load moves one step downward and new materials enters the reactor from the top. Outlet temperature shows limited periodic variations and the solid flow control actuator remains simple compared to a fully continuous technology.

Tests were conducted on a dynamically controlled air flow equipment, where a calibrated instrumentation allowed to measure thermal power with temperature and humidity methods, in addition to mass gradients. Comprehensive measurements with consistent results showed that the reactor was well designed with low thermal losses and good air tightness. In addition, this validated the measurement methods and the understanding of the thermochemical concepts. The reactor was tested in both heating and storage modes for Brussels climate under 5 different operating conditions representing winter, mid-season, summer and intermediate cases, with 16 m² of flat panel solar thermal collectors. Three additional heating cases were measured in order to evaluate air flow influence.

A first algorithm was developed for controlling the semi continuous solid flow, which allowed to run the tests. However, it was highlighted that monitoring solid hydration level in real time would definitely help managing the reaction, and that a volumetric valve would be more appropriate than a time based valve. It was also shown that the reactor requires an initialization period, during which its behavior is quite different from continuous operation. The energy density being lower, initialization occurrence has to be minimized.

The reactor heating (or hydration) power is highly influenced by inlet humidity ratio: it reaches 215 W at 3.9 g/kg_{da} and 415 W at 9 g/kg_{da}, according to stabilized measurements with both temperature and humidity methods. The coefficient of performance is very high (19 to 45), which confirms that auxiliary power is quite low. In addition, it was measured that doubling the air flow rate multiplies heating power by 2.1 and divides coefficient of performance by 1.9. As a consequence, reaction power can be easily adjusted by controlling fan speed, with the limit of electrical consumption. A 16-points temperature map located at reactor outlet's sieve showed a downward decreasing gradient, which confirmed the theoretical approach, where dryer upper composite reacts faster. This enlarges the potential functionalities of the temperature map, as we see that solving a heat equation system would allow to estimate solid material hydration level in several reactor locations. Without real time hydration level, energy density was rather estimated and may be inaccurate. Nevertheless, it seems to be lower than expected because of reaction control issues that shortened the tests. Conversely, an optimal test duration would likely lead to slightly lower averaged heat power.

The reactor heat storing (or dehydration) power reaches 385 W at 60.3°C and 415 W at 90.9°C. Because of a higher temperature, stabilization time is much longer than for heating mode. Due to a limited quantity of prepared solid composite, dehydration analysis had to be performed before full continuous operation occurs, which means with less accuracy. As for heating mode, tests were shortened because of reaction control issues. Thermal power increases with temperature and decreases with specific humidity, it remains high and stable even at solar heat favorable temperature, which is a major result for energy efficient storage systems. Some reactor clogging occurred and was confirmed by a warmer left column on the outlet temperature map, meaning a lower composite

flow in this section. As for heating mode, there was an excellent heat power correlation between temperature and humidity methods, which means that the specific humidity measurement setup compensates the lack of accuracy at higher temperature. This lead to an appropriate measurement of the physical phenomenon involved in a prototype that minimizes air leaks and thermal losses.

6. Acknowledgment

This research was performed within the SoTherCo project, which has received funding from the European Union's Seventh Framework Programme for research, technological development and demonstration under grant agreement n°295775.

7. References

Bonk, S., Kerskes, H., Drück, H., 2017. Development and testing of a thermo-chemical energy store - Results of a five year research project. Presented at the ISES Solar World Congress 2017 - IEA SHC International Conference on Solar Heating and Cooling for Buildings and Industry 2017, Proceedings, pp. 695–704. https://doi.org/10.18086/swc.2017.13.01

Courbon, E., D'Ans, P., Permyakova, A., Skrylnyk, O., Steunou, N., Degrez, M., Frère, M., 2017. A new composite sorbent based on SrBr2 and silica gel for solar energy storage application with high energy storage density and stability. Appl. Energy 190, 1184–1194. https://doi.org/10.1016/j.apenergy.2017.01.041

Courbon, E., Frère, M., Heymans, N., D'Ans, P., 2015. Hygroscopic composite material. WO 2015 197788 A1.

Kerskes, H., Mette, B., Bertsch, F., Asenbeck, S., Drück, H., 2012. Chemical energy storage using reversible solid/gas-reactions (CWS) – results of the research project. Energy Procedia, 1st International Conference on Solar Heating and Coolingfor Buildings and Industry (SHC 2012) 30, 294–304. https://doi.org/10.1016/j.egypro.2012.11.035

Letz, T., 2002. Validation and Background Information on the FSC Procedure (IEA Task 26 - Reports of Subtask A).

Marias, F., 2015. Seasonal storage of solar energy by thermochemical reactions at atmospheric pressure for household applications. PhD Thesis, Université de Grenoble.

Mauran, S., Lahmidi, H., Goetz, V., 2008. Solar heating and cooling by a thermochemical process. First experiments of a prototype storing 60kWh by a solid/gas reaction. Sol. Energy 82, 623–636. https://doi.org/10.1016/j.solener.2008.01.002

Mette, B., Kerskes, H., Drück, H., 2014. Experimental and numerical investigations of different reactor concepts for thermochemical energy storage. Presented at the Energy Procedia, pp. 2380–2389. https://doi.org/10.1016/j.egypro.2014.10.246

Michel, B., Mazet, N., Mauran, S., Stitou, D., Xu, J., 2012. Thermochemical process for seasonal storage of solar energy: Characterization and modeling of a high density reactive bed. Energy, Asia-Pacific Forum on Renewable Energy 2011 47, 553–563. https://doi.org/10.1016/j.energy.2012.09.029

Michel, B., Mazet, N., Neveu, P., 2016. Experimental investigation of an open thermochemical process operating with a hydrate salt for thermal storage of solar energy: Local reactive bed evolution. Appl. Energy 180, 234–244. https://doi.org/10.1016/j.apenergy.2016.07.108

Nonnen, T., Beckert, S., Gleichmann, K., Brandt, A., Unger, B., Kerskes, H., Mette, B., Bonk, S., Badenhop, T., Salg, F., Gläser, R., 2016. A Thermochemical Long-Term Heat Storage System Based on a Salt/Zeolite Composite. Chem. Eng. Technol. 39, 2427–2434. https://doi.org/10.1002/ceat.201600301

Van Helden, W., Wagner, W., Schubert, V., Krampe-Zadler, C., Kerskes, H., Mette, B., Jänchen, J., 2014. First tests on a solid sorption prototype for seasonal solar thermal storage. Presented at the Thermische Solarenergie, Staffelstein, Germany.